Environmental Science & Technology

Article

Cite This: Environ. Sci. Technol. 2018, 52, 397−405

pubs.acs.org/est

Aerosol Emissions from Great Lakes Harmful Algal Blooms

Nathaniel W. May,[†] Nicole E. Olson,[†] Mark Panas,[†] Jessica L. Axson,[‡] Peter S. Tirella,[†] Rachel M. Kirpes,[†] Rebecca L. Craig,[†] Matthew J. Gunsch,[†] Swarup China,[§] Alexander Laskin,[§,⊥] Andrew P. Ault,*[,†,‡] and Kerri A. Pratt*[,†,∥]

[†]Department of Chemistry, University of Michigan, Ann Arbor, Michigan, United States

[‡]Department of Environmental Health Sciences, University of Michigan, Ann Arbor, Michigan, United States

[§]William R. Wiley Environmental Molecular Sciences Laboratory, Pacific Northwest National Laboratory, Richland, Washington, United States

[∥]Department of Earth and Environmental Sciences, University of Michigan, Ann Arbor, Michigan, United States

Supporting Information

ABSTRACT: In freshwater lakes, harmful algal blooms (HABs) of *Cyanobacteria* (blue-green algae) produce toxins that impact human health. However, little is known about the lake spray aerosol (LSA) produced from wave-breaking in freshwater HABs. In this study, LSA were produced in the laboratory from freshwater samples collected from Lake Michigan and Lake Erie during HAB and nonbloom conditions. The incorporation of biological material within the individual HAB-influenced LSA particles was examined by single-particle mass spectrometry, scanning electron microscopy with energy-dispersive X-ray spectroscopy, and fluorescence microscopy. Freshwater with higher blue-green algae content produced higher number fractions of individual LSA particles that contained biological material, showing that organic molecules of biological origin are incorporated in LSA from HABs. The number fraction of individual LSA particles containing biological material also increased with particle diameter (greater than 0.5 μm), a size dependence that is consistent with previous studies of sea spray aerosol impacted by phytoplankton blooms. Similar to sea spray aerosol, organic carbon markers were most frequently observed in individual LSA particles less than 0.5 μm in diameter. Understanding the transfer of biological material from freshwater to the atmosphere via LSA is crucial for determining health and climate effects of HABs.

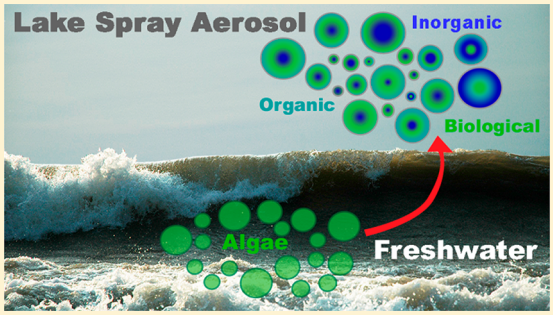

INTRODUCTION

Eutrophication of freshwater resulting from increased anthropogenic nutrient loading has led to a global increase in harmful algal blooms (HABs), which are typically caused by *Cyanobacteria* (blue-green algae).[1] Biogenic organic toxins (e.g., microcystis) contained within, and introduced into the aquatic environment by, blue-green algae (BGA) are a threat to both human and animal health through direct ingestion.[2] Marine wave breaking under HAB conditions introduces toxic marine HAB products into the atmosphere alongside sea spray aerosol (SSA), with air concentrations of toxins as low as 2−7 ng m^{-3} inducing upper respiratory symptoms,[3,4] suggesting the same process could occur in freshwater. Since freshwater recreational activity aerosolizes toxic HAB products (0.1−0.4 ng m^{-3}),[5,6] it is likely that freshwater wave breaking producing lake spray aerosol (LSA) under HAB conditions may be a previously unrecognized exposure route for HAB toxins. However, the only previous measurements of LSA chemical composition, which showed that the inorganic composition of LSA is reflective of freshwater, occurred during a period of low biological activity in Lake Michigan.[7] As a result, there is currently a lack of understanding of how freshwater HABs affect the incorporation of biological material in LSA.

The relationship between seawater composition and SSA[8,9] can inform our currently limited understanding of the links between the compositions of freshwater and LSA. Organics present in SSA are enriched relative to bulk seawater due to two mechanisms in the bubble bursting particle production method. Hydrophobic organic matter first accumulates at the surface of bubbles as they rise through the water column,[10−13] and then organics in the sea surface microlayer (60 μm thick)[14] are added to the bubble surface.[15] The concentration of organics at the bubble surface is then translated to an enrichment of organics in particles formed from droplets produced from the fragmentation of the bubble film cap.[16] It is likely, given that organic material is also concentrated in films at the surface of freshwater (100 μm thick),[17−19] that LSA also become enriched in organics relative to bulk freshwater concentrations through

Received: July 15, 2017
Revised: November 22, 2017
Accepted: November 24, 2017
Published: November 24, 2017

DOI: 10.1021/acs.est.7b03609
Environ. Sci. Technol. 2018, 52, 397−405

the same mechanisms identified for SSA. Dissolved organic content in freshwater without algal blooms (10−180 μM C)[20−22] and with algal blooms (400 μM C)[23] is similar in concentration to seawater without and with algal blooms (80 and 50−300 μM C, respectively).[22,24,25] The lower inorganic ion concentration in freshwater (0.05−0.15 g L^{-1})[26] compared to seawater (35 g L^{-1})[25] results in a higher ratio of organic to inorganic content in freshwater compared to seawater.[27] Therefore, organics may comprise a larger fraction by mass in LSA compared to SSA, likely impacting particle hygroscopicity and reactivity.[28,29] The enrichment of organics in particles affects cloud condensation nuclei (CCN) activity of SSA, and possibly of LSA, as the addition of less water-soluble organic species to salt particles decreases the overall hygroscopicity and increases the diameter at which particles can activate as CCN.[29] In addition, organic compounds and biological material aerosolized from marine algal blooms by bubble bursting[30−32] contribute to marine ice nucleating particle (INP) populations,[32−36] and organic compounds and biological material aerosolized from freshwater algal blooms may do the same in freshwater environments. Furthermore, biological species in freshwater with the potential to act as INP[37] are two to three orders of magnitude higher concentration in than in seawater.[38] These potential climate impacts of LSA may be reduced, compared to SSA, by the lower concentration of particles produced from bubble-bursting in freshwater compared to seawater.[27] However, the distribution of organic and biological material across the population of bubble bursting particles (i.e., mixing state) plays an important role in determining their climate properties.[9,39−41]

Blue-green algae are the most widespread and common cause of HABs in the Laurentian Great Lakes of North America and have become increasingly important due to their significant resurgence near population centers.[2,42] The Great Lakes are characterized by large surface area, frequent high wind speeds, and significant fetch, leading to extensive wave breaking, which is conducive to LSA production.[43] LSA with variable biological content could be produced throughout the region due to the variability in the BGA concentration across the Great Lakes.[2] Since the Laurentian Great Lakes system is a contiguous body of water, the effect of blue-green algae concentrations on LSA composition can be examined using samples collected from different lakes because of their similar inorganic ion composition.[26] In this study, freshwater samples were collected from Lake Erie and Lake Michigan from three locations with varying levels of BGA.[44] The freshwater samples were used to generate LSA in the laboratory using a recently constructed laboratory LSA generator with a plunging jet system[27] that produces particles analogous to natural wave-breaking.[45] Individual particles were analyzed using single-particle mass spectrometry and microscopy to determine size-resolved chemical composition. Chemical signatures of individual LSA particles were identified based on inorganic, organic, and biological ion markers. For each of the three freshwater samples, the relationship between freshwater BGA concentration and LSA chemical composition was examined. Fluorescence microscopy provided additional confirmation of the incorporation of biological material within individual particles. This information can be used for future identification of atmospheric LSA produced from freshwater of varying HAB content through field studies.

EXPERIMENTAL METHODS

Freshwater Sample Collection and Aerosol Generation. Freshwater was collected from the top ∼5 cm of the surface of three Great Lake sites in 8 L LDPE carboys. The three samples and corresponding collection times were as follows: (1) Lake Erie - Maumee Bay State Park, Oregon, Ohio (N 41.686365, W −83.372286) collected on September 12, 2014, (2) Lake Erie - Catawba Island State Park, Port Clinton, Ohio (N 41.573131, W −82.857192) collected on September 12, 2014, and (3) Lake Michigan − Washington Park Beach, Michigan City, Indiana (N 41.727573, W −86.909516) collected on October 12, 2014. An additional freshwater sample was collected from the Lake Erie - Maumee location on September 20, 2017 to test the effect of freshwater sample freezing on LSA composition. Figure 1 shows the sampling

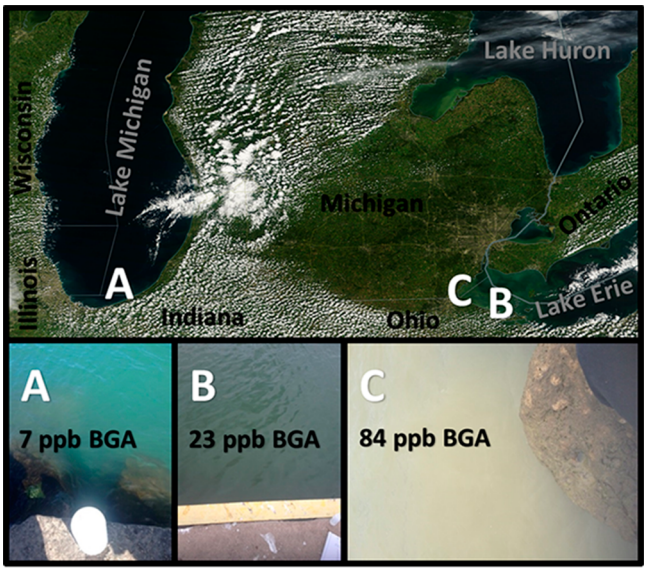

Figure 1. NASA MODIS satellite image of the Great Lakes region on September 17, 2014 with locations marked for Great Lakes surface freshwater sampling: (A) Lake Michigan - Michigan City, (B) Lake Erie - Catawba, and (C) Lake Erie - Maumee, with corresponding photographs of surface freshwater, with measured blue green algae concentrations inset.

locations on a NASA MODIS satellite image from September 17, 2014, the nearest clear sky day that allowed for a full visualization of the Great Lakes; photographs of the surface freshwater at the three sites at the time of collection are also shown. For comparison, Supporting Information (SI) Figure S1 shows NASA MODIS satellite images from October 12, 2014 and September 22, 2017, the nearest clear sky days that allowed for a full visualization of the Great Lakes; a photograph of the September 20, 2017 Lake Erie − Maumee surface freshwater is also shown. During freshwater sampling, a hand-held spectrophotometer (AquaFluor 8000) measured BGA content through phycocyanin fluorescence, which serves as an indicator for algal cell and microcystin concentrations.[44]

The three 2014 freshwater samples were frozen (−20 °C) after sampling for storage over a period of 20 months and thawed prior to aerosol generation in a laboratory LSA generator. Half of the 2017 Lake Erie - Maumee freshwater sample was used for aerosol generation in the laboratory LSA generator on the day of collection. The other half of the 2017 Lake Erie - Maumee freshwater sample was frozen (−20 °C)

DOI: 10.1021/acs.est.7b03609
Environ. Sci. Technol. 2018, 52, 397−405

after sampling for storage over a period of 24 h and thawed prior to aerosol generation in the laboratory LSA generator. Details of the LSA generator construction, operation, and validation studies are provided by May et al.[27] Briefly, the LSA generator circulates 4 L of freshwater sample at 2 L min^{-1} via a diaphragm pump into four plunging jets, which creates bubbles that burst at the freshwater sample surface to generate aerosol particles. During all experiments the tank was kept at room temperature (23 ± 1 °C) with a relative humidity (RH) of 85%. Generated freshwater aerosols were passed through two silica gel diffusion dryers to achieve a RH of ∼15% before measurement to reduce the suppression of negative ion formation by particle phase water in the single-particle mass spectrometer.[46] Prior to particle generation, particle-free air (Pall, HEPA Capsule Filter) was cycled through the LSA generator. Background particle concentrations were negligible (<20 particles cm^{-3}; < 5%), in comparison to the average total particle concentration generated from the freshwater samples (∼750 particles cm^{-3}), and below sizes (d_a < 250 nm) chemically analyzed by single particle techniques. The aerosol number size distributions and total aerosol concentrations (SI Figure S2) for each LSA sample were measured by a scanning mobility particle sizer (SMPS), consisting of a differential mobility analyzer (DMA; TSI Inc., model 3082) and a CPC (TSI Inc., model 3775) for particles with electrical mobility diameters (d_m) between 14.1 and 736.5 nm, as well as an aerodynamic particle sizer (APS; TSI Inc., model 3321) for particles with aerodynamic diameters (d_a) between 0.52 and 19.8 μm.

Single Particle Analysis. An aerosol time-of-flight mass spectrometer (ATOFMS) was used for the real-time analysis of the size and chemical composition of individual LSA particles ranging from vacuum aerodynamic diameters of 0.25−1.5 μm.[47] Briefly, particles enter the instrument through an aerodynamic focusing lens creating a narrow particle beam. Particles are then accelerated to terminal velocities, which are measured by the time a particle takes to pass between two continuous wave lasers, with wavelengths of 488 and 405 nm, respectively, separated by 6 cm. Particle aerodynamic diameter is obtained by calibrating size dependent particle terminal velocity using polystyrene latex spheres of known diameter (0.1−2.5 μm) and density (1 g/cm^3). Individual particles entering the mass spectrometer are desorbed and ionized by a 266 nm Nd:YAG laser (1.2 mJ) generating positive and negative ions. Ions are detected using a dual polarity time-of-flight mass spectrometer. All particle measurements discussed here describe nascent LSA, sampled less than 10 s following production, thus minimizing subsequent chemical processing of these particles. 8857 particles were chemically analyzed by ATOFMS for the 2014 Lake Michigan - Michigan City sample, 11 407 particles for the 2014 Lake Erie - Maumee sample, and 9827 particles for the 2014 Lake Erie - Catawba sample. 4651 particles were chemically analyzed by ATOFMS for the 2017 Lake Erie - Maumee sample prefreeze experiment and 5255 particles for the 2017 Lake Erie - Maumee sample post-freeze experiment. Mass spectral peak identifications correspond to the most probable ion(s) for a given m/z ratio based on previous studies.[7,9,40,48] Relative peak area searches for combinations of inorganic, organic, and biological marker ions within single-particle mass spectra were completed using the MATLAB toolkit FATES (Flexible Analysis Toolkit for the Exploration of Single-particle mass spectrometry data)[49] to identify and separate the distinct single-particle types observed. The effect of the freeze−thaw process on the observed individual particle chemical composition is described in the Supporting Information (SI).

A microanalysis particle sampler (MPS, California Measurements, Inc.) impacted particles from the three 2014 freshwater samples onto Formvar coated copper microscopy grids (Ted Pella, Inc.) for analysis by scanning electron microscopy (SEM) and onto aluminum foil for fluorescence analysis. The MPS is operated at 2 L min^{-1} and consists of 3 stages with aerodynamic diameter size cuts of 2.5−5.0 μm for stage 1, 0.7−2.5 μm for stage 2, and <0.7 μm for stage 3. Particles collected on stage 3 of the MPS were analyzed using a Quanta environmental scanning electron microscope (ESEM, FEI). The FEI Quanta was operated at 20 kV and used a high angle annular dark field (HAADF) detector and an EDAX energy dispersive X-ray spectroscopy (EDX) detector to collect images and EDX spectra of 30 individual particles, respectively. In addition, particle circularity distributions were determined using SEM for 1250 particles from the Lake Michigan - Michigan City sample, 2016 particles from the Lake Erie - Catawba sample, and 1766 particles from the Lake Erie - Maumee sample, from stages 2 and 3 of the MPS.

Particles from the three 2014 freshwater samples collected on stage 2 of the MPS were analyzed with a Raman microspectrometer (Horiba LabRAM HR Evolution) with a confocal microscope (100× objective) and a Nd:YAG laser (532 nm, 50 mW) for fluorescence analysis. The Raman spectrometer was operated in Swift mode with a 600 groove/mm grating and used a CCD detector. Fluorescence spectra were acquired from 545 to 605 nm over an area of 50 × 53 μm with a step size of 0.5 μm using 0.1 s acquisitions to create fluorescence maps of individual particles. Representative fluorescence maps of individual particles for each sample are shown in SI Figure S3. The summed fluorescence intensities of 5 maps, each with ∼20 particles, for each sample were averaged together and normalized to the highest average fluorescence intensity sample.

RESULTS AND DISCUSSION

LSA Particle Chemical Composition & Morphology. Three distinct individual types of particles were identified by ATOFMS from the LSA generated in the laboratory from the freshwater surface samples. These three individual particle types are identified as LSA primarily composed of inorganic salts (LSA-Salt), LSA with elevated organic carbon content (LSA-Organic), and LSA with biological material (LSA-Bio). This classification of LSA particle types is consistent with previous single particle mass spectrometry studies of laboratory generated SSA, which defined particle types on a scale of increasing organic and biological content: sea salt (SS), sea salt with organic carbon (SS-OC), bioparticles (Bio), and organic carbon (OC).[9,40,50] The seawater-sourced OC particles are typically smaller in diameter (<0.2 μm)[40] than the lower size limit (0.25 μm) of the ATOFMS used in this study, such that freshwater-sourced OC particles may not be expected to be detected herein, as observed. Average dual polarity mass spectra from all three freshwater samples are shown for each of the three particle types, with major ions labeled, in Figure 2. Difference mass spectra, calculated as the difference between the average mass spectra between pairs of particle types, highlight the major changes in composition between the three particle types and are shown in SI Figure S4.

DOI: 10.1021/acs.est.7b03609
Environ. Sci. Technol. 2018, 52, 397−405

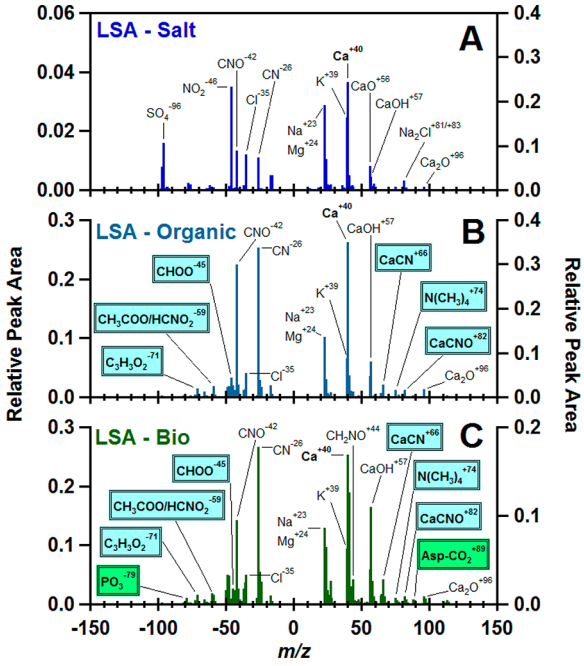

Figure 2. Average negative (left) and positive (right) ion mass spectra of individual particles defined as (A) LSA-Salt, (B) LSA-Organic, and (C) LSA-Bio. Ions significantly enhanced in LSA-Organic and LSA-Bio, compared to LSA-Salt, particles are highlighted in blue, and ions significantly enhanced in LSA-Bio, compared to LSA-Organic and LSA-Salt, particles are highlighted in green; for comparison, mass spectral difference plots are shown in SI Figure S4.

The individual LSA-Salt particle mass spectra were characterized by m/z 40 [Ca^+] as the highest intensity peak (Figure 2A), reflective of calcium as the highest concentration cation in Great Lakes freshwater[26] and consistent with previous ATOFMS analyses of LSA generated from Lake Michigan freshwater with low BGA concentration (11 ppb).[7] Minor inorganic ion peaks included m/z + 23 [Na^+], + 24 [Mg^+], + 39 [K^+], and +56 [CaO^+]. The LSA-Salt particle mass spectra were further defined by the lack of significant organic ions in the positive ion mass spectra. The LSA-Salt particle type negative ion mass spectrum was characterized by m/z −26 [CN^-] and −42 [CNO^-], representative of organic nitrogen,[40] as the most prominent peaks, consistent with our previous ATOFMS study of laboratory generated LSA from a Lake Michigan freshwater sample.[7]

The individual LSA-Organic particle mass spectra (Figure 2B) exhibited similar inorganic ions as the LSA-Salt particle mass spectra, again with m/z + 40 [Ca^+] as the most prominent peak in the positive ion mass spectrum. However, the LSA-Organic particle mass spectra were differentiated from the LSA-Salt particle mass spectra by the presence of significant m/z + 66 [$CaCN^+$] and +82 [$CaCNO^+$] peaks, consistent with enhanced organic nitrogen content.[40] Additional significant organic ions were detected: m/z + 74 [$N(CH_3)_4^+$], −45 [$CHOO^-$], −59 [CH_3COO^-], and −71 [$C_3H_3O_2^-$] (Figure 2).[48] Therefore, similar to the classification of ATOFMS particles in SSA studies, the LSA-Organic particles are similar to the LSA-Salt particles, but with an enrichment in organic carbon internally mixed with the salt particles.[9,40]

The individual LSA-Bio particles (Figure 2C) exhibited similar organic and inorganic ions as the LSA-Organic particle mass spectra. However, as shown in the mass spectral difference plots (SI Figure S4) and highlighted in Figure 2, the LSA-Bio particles were distinguished from the LSA-Salt and LSA-Organic particles by the significant presence of m/z + 89, suggested to be the common amino acid aspartic acid observed as [Asp−CO_2], based on previous bioaerosol studies.[51] The LSA-Bio particle mass spectra were further defined by the presence of a significant phosphate ion peak (m/z −79 [PO_3^-]) (SI Figure S4), which previous ATOFMS studies have found to be unique to particles containing primary biological material, when combined with organic nitrogen ion markers (m/z −26 [CN^-] and −42 [CNO^-]).[40,52,53] Similar to the established marine biological aerosol mass spectral signature,[40] this LSA-Bio mass spectral signature likely represents fragments of BGA cells, which are typically 3−7 μm,[54] as well as BGA exudates. Therefore, the LSA-Bio particles could potentially contain toxins from the BGA measured in the freshwater samples. Future measurements to differentiate between toxic and nontoxic biological species in particles are needed to assess the toxicity and public health impacts of the individual LSA-Bio particles.

The identification of the LSA-Salt, LSA-Organic, and LSA-Bio particles by ATOFMS was complemented by EDX analyses of single particle elemental composition (Figure 3). The EDX

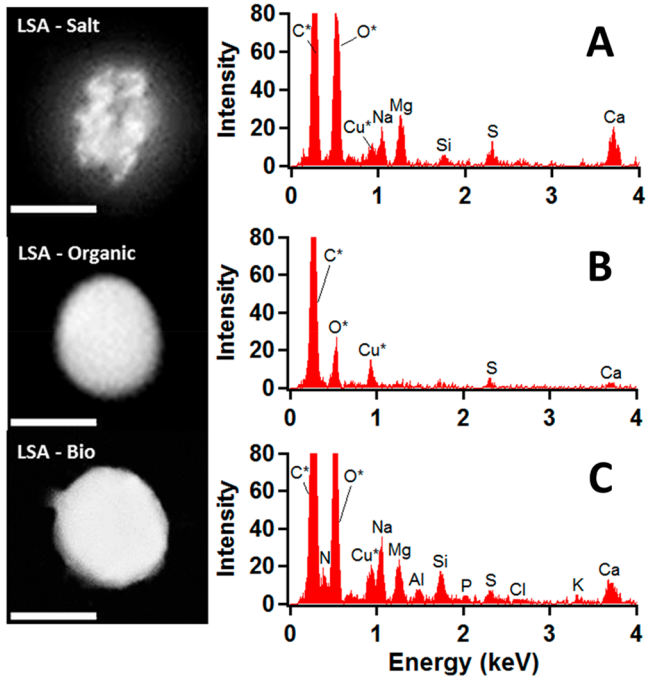

Figure 3. Scanning electron microscopy images with 1 μm scale bars (left) and corresponding energy dispersive X-ray spectra (right) of representative individual particles defined as (A) LSA-Salt, generated from the 2014 Lake Michigan − Michigan City freshwater sample, (B) LSA-Organic, generated from the 2014 Lake Michigan−Michigan City freshwater sample, and (C) LSA-Bio, generated from the 2014 Lake Erie−Maumee freshwater sample.

spectrum of a representative LSA-Salt particle was characterized by inorganic elements Na and Mg, with Ca as the highest intensity peak (Figure 3A), consistent with the ATOFMS mass spectra (Figure 2) and Great Lakes freshwater composition.[26] This Ca-dominant elemental composition and cubic morphology is similar to previous SEM-EDX analyses of ambient LSA collected on the coast of Lake Michigan and LSA generated in the laboratory from Lake Michigan freshwater of low BGA

DOI: 10.1021/acs.est.7b03609
Environ. Sci. Technol. 2018, 52, 397−405

concentration.[7] The EDX spectrum of a LSA-Organic particle was also characterized by Ca as the highest intensity peak (Figure 3B), consistent with the LSA-Organic ATOFMS mass spectra (Figure 2) and Great Lakes freshwater;[26] however, this particle had lower relative contributions from other inorganic elements present in the EDX spectra of LSA-Salt particles. While the carbon peak in the EDX spectrum is partly due to contributions from the microscopy substrate, the lack of other elements present suggests that carbon and oxygen from organic compounds comprised a significant fraction of the LSA-Organic particle mass. The LSA-Bio particle was further differentiated from the LSA-Organic particle by the presence of N and P, known markers of biological content,[55] in the EDX spectra (Figure 3C) and consistent with the ATOFMS spectra.

The identification of the individual LSA-Salt, LSA-Organic, and LSA-Bio particles by EDX analysis of single particle elemental composition was further supported by SEM analysis of single particle morphology (Figure 3). The LSA-Salt particle was defined in SEM images by a cubic core surrounded by a circular shell, the result of water loss from the particle after deposition to form a salt crystal.[56] Increased total organic carbon concentration in seawater has been shown to disrupt the crystallization of salts in SSA during drying on the substrate resulting in more circular particles.[56] In addition, previous SEM analysis demonstrated that LSA generated from Lake Michigan freshwater exhibited increased circularity compared to LSA generated from a synthetic freshwater representative of Great Lakes inorganic ion content without organic content.[27] Therefore, the increased circularity of the LSA-Organic particle type observed in the SEM image, in comparison to the LSA-Salt particle type, further supports the increased incorporation of organic carbon identified by EDX analysis. The LSA-Bio particle type exhibited similar circularity to the LSA-Organic particle type, which is consistent with transmission electron microscopy studies of laboratory generated SSA that found biological particles to be circular.[57]

Effect of Blue Green Algae Content on LSA Composition. A direct relationship was observed between the BGA content of the 2014 surface freshwater samples and the submicrometer and supermicrometer ATOFMS number fractions of individual LSA-Bio particles (Figure 4). The low biological activity Lake Michigan−Michigan City sample (7 ppb BGA) produced the lowest LSA-Bio submicrometer (1 ± 1% (standard error)) and supermicrometer (3 ± 1%) particle number fractions. The Lake Erie−Catawba sample, which had the second highest biological activity (23 ppb BGA), produced the second highest submicrometer (11 ± 1%) and supermicrometer (34 ± 1%) number fractions of LSA-Bio particles. The highest biological activity Lake Erie−Maumee sample (84 ppb BGA) produced the correspondingly highest submicrometer (17 ± 1%) and supermicrometer (44 ± 1%) particle number fractions of LSA-Bio particles. While the measured BGA concentration did not change after freezing and thawing the freshwater, an 8% decrease in the number fraction of LSA-Bio particles and corresponding 10% increase in the number fraction of LSA-Organic particles were observed for the moderate biological activity Lake Erie−Maumee 2017 sample (40 ppb BGA); these changes in LSA composition were likely due to the release of organic material from cell lysis during the freeze−thaw process, as discussed in the SI. Therefore, while future studies should avoid freezing freshwater when possible to avoid biasing the number fraction of individual LSA-Organic particles high and biasing the number fraction of LSA-Bio particles low, this did not impact the overarching trends observed in this study. In addition, a similar positive association between seawater biological content and SSA biological particle type number fraction was shown in a laboratory SSA generation study, where increasing seawater biological content (chlorophyll-a: 0.5−5 mg/m^3; heterotrophic bacteria 1 × 10^6 to 7 × 10^6 cells/mL) corresponded to the SSA-Bio number fraction increasing from 18% to 30% (using ATOFMS to probe 0.5−3.0 μm particles).[40] Therefore, the increase in the number fractions of individual LSA-Bio particles with increasing measured BGA concentration further demonstrates the incorporation of biological material in LSA.

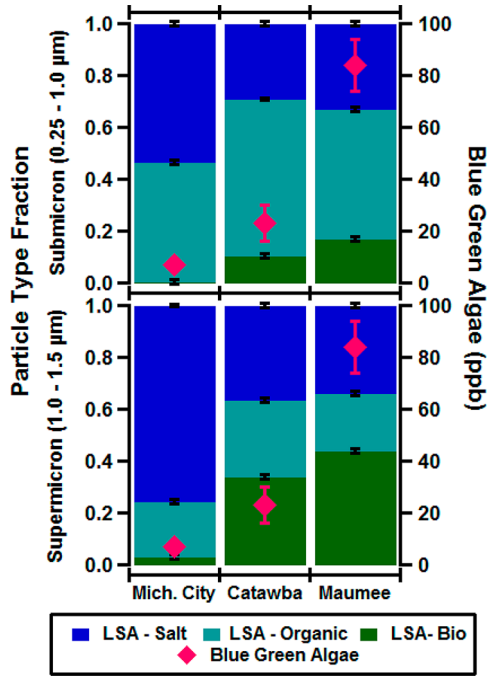

Figure 4. Number fractions of ATOFMS particle types, with standard errors shown, for submicrometer (0.25−1.0 μm) (top) and supermicron (1.0−1.5 μm) (bottom) particles generated in the laboratory from freshwater samples collected in 2014 from Lake Michigan−Michigan City (left), Lake Erie−Catawba (center), and Lake Erie−Maumee (right). Average blue green algae concentrations, with standard deviations shown, of the freshwater samples measured at the time of collection are also shown.

As shown in Figure 5, similar size dependence was observed in the number fractions of LSA-Bio and LSA-Salt particles produced by the three 2014 freshwater samples. For the elevated biological content Lake Erie−Catawba (23 ppb) and Lake Erie−Maumee (84 ppb) freshwater samples, the number fraction of individual LSA-Bio particles increased substantially as particle diameters increased from 0.4 to 1.5 μm (1% to 40% and 3% to 50%, respectively). While evident, this increase was less substantial for the low biological content (7 ppb) Lake Michigan−Michigan City freshwater sample, with the number fraction of individual LSA-Bio particles increasing from 0.6% to 6% for particle diameters from 0.4 to 1.5 μm. Consistent with this size-dependent trend, previous ATOFMS measurements of laboratory generated SSA from an induced phytoplankton bloom observed the greatest contribution of biological aerosols at supermicrometer diameters,[9,39,53] which was attributed to the enrichment of biological material in marine jet drops.[58] Since the LSA-Bio particles primarily exist at larger diameters resulting from freshwater jet drops,[27] the jet drop aerosol

DOI: 10.1021/acs.est.7b03609
Environ. Sci. Technol. 2018, 52, 397−405

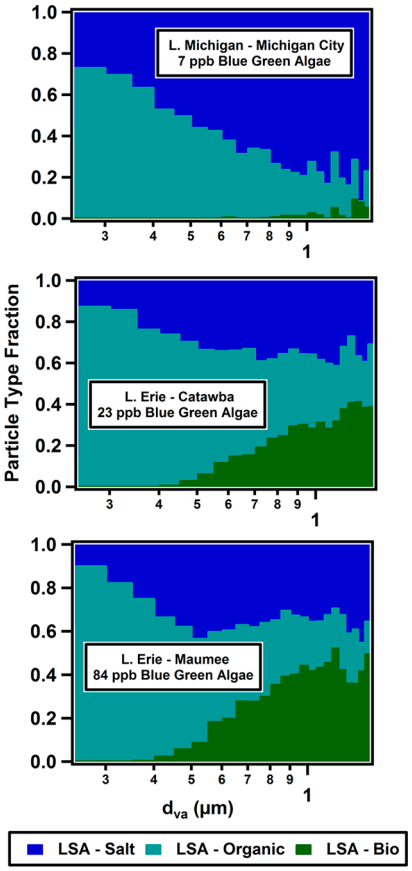

Figure 5. Size-resolved (0.25−1.5 μm) particle type number fractions measured by ATOFMS for particles generated in the laboratory from freshwater samples collected in 2014 from Lake Michigan−Michigan City (top), Lake Erie−Catawba (middle), and Lake Erie−Maumee (bottom).

generation process likely leads to the enrichment of biological material within LSA, similar to SSA. Following a similar process, LSA-Salt particles were also primarily observed in particles at larger diameters, regardless of freshwater sample (Figure 5 and S6). For the low biological content (7 ppb BGA) Lake Michigan−Michigan City freshwater sample, the LSA-Salt particle number fraction increased substantially as particle diameters increased from 0.25 to 1.5 μm (26% to 76%). A previous ATOFMS study of laboratory generated SSA observed a comparable increase in inorganic-rich sea salt particles as particle diameters increased from 0.55 to 3 μm.[9,39] The increase in the number fraction of inorganic-rich aerosols at larger diameters in both SSA and LSA is attributed to their production by jet drops,[59] which are larger and more representative of the inorganic-rich bulk solution than film drops.[60]

The size dependence of LSA-Organic particle number fractions produced from all three 2014 freshwater samples, characterized by greater contributions to smaller particles, is distinct from the size dependence of LSA-Salt and LSA-Bio particles. The LSA-Organic particle number fraction decreased as particle diameters increased from 0.25 μm (Lake Michigan−Michigan City = 74%; Lake Erie−Catawba = 88%; Lake Erie−Maumee = 90%) to 1.5 μm (Lake Michigan−Michigan City = 18%; Lake Erie−Catawba = 30%; Lake Erie−Maumee = 15%) for all three 2014 freshwater samples (Figure 4), similar to studies of laboratory generated SSA that observed a decrease in SSA-Organic particle type number fractions from 0.3 to 1.5 μm in diameter.[9] In the marine environment, smaller particles resulting from film drops in the bubble bursting process are enriched in organic compounds due to the high concentration of organics at the surface of seawater and bubbles.[60] Therefore, an increase in the LSA-Organic particle number fractions at smaller particle diameters is consistent with an enrichment in organics at the surface of freshwater,[17−19] leading to an enrichment in smaller LSA particles resulting from the freshwater bubble bursting process. All freshwater samples produced higher total number fractions (46−60%) of LSA-Organic particles, compared to the total number fractions (23−27%) of SSA-Organic particles generated from subsurface seawater enriched in organic material by a laboratory induced phytoplankton bloom.[39] This is likely due to the higher proportion of organic material relative to inorganic material present in freshwater,[20−22,26] compared to seawater, even under phytoplankton bloom conditions.[22,25] Particle circularity distributions (measured from SEM images), shown in SI Figure S7, demonstrate that, for all three freshwater samples, the distribution maximum was close to 1, indicative of primarily spherical particles. These data are consistent with circularity distributions of particles previously generated from a Lake Michigan freshwater sample[27] and suggest that all of the freshwater samples are comprised of sufficient organic matter to disrupt cubic crystal formation within the LSA.[27,56]

Normalized average fluorescence intensity derived from fluorescence microspectroscopy mapping of impacted particles (Figure 6 and SI Figure S3) further suggests a direct

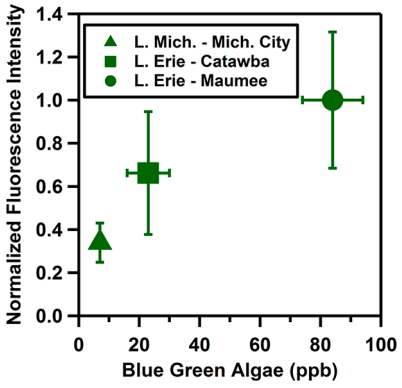

Figure 6. Normalized fluorescence intensity, an indicator of biological content, for particles generated from the Lake Michigan−Michigan City, Lake Erie−Catawba, and Lake Erie−Maumee freshwater samples collected in 2014, as a function of blue green algae concentrations of the freshwater samples at the time of collection. Error bars shown are standard deviations.

relationship between the increased contributions of individual LSA-Bio particles with measured BGA concentration. For the lowest BGA concentration (7 ppb) Lake Michigan−Michigan City freshwater sample, the lowest normalized average fluorescence intensity (0.34 ± 0.09 (standard deviation)) was observed. The Lake Erie−Catawba freshwater sample (23 ppb BGA) was characterized by an intermediate normalized average fluorescence intensity (0.7 ± 0.3), and the Lake Erie−Maumee freshwater sample, with the highest BGA concentration (84 ppb), exhibited the highest normalized average fluorescence intensity (1.0 ± 0.3). While a statistically significant increase in fluorescence intensity of particles was only observed between the lowest (7 ppb BGA) and highest (84 ppb BGA) biological

DOI: 10.1021/acs.est.7b03609
Environ. Sci. Technol. 2018, 52, 397−405

content samples, it is supportive of the statistically significant increase in the LSA-Bio particle number fractions with increasing freshwater BGA concentration, and provides further evidence of the bubble bursting production of bioaerosols from freshwater environments, with a dependence on biological activity. The increased fluorescence of particles associated with increased BGA concentration is indicative of increased biological particle content as organic molecules of biological origin, such as proteins and coenzymes, exhibit intrinsic fluorescence, providing a means for bioaerosol detection.[50,61]

Atmospheric Implications. This study examined the individual particle chemical composition of LSA generated from freshwater of varying BGA content. Individual LSA particles primarily composed of inorganic salts, inorganic salts with organic compounds, and inorganic salts with biological material were identified, with the biological content of individual LSA particles increasing with freshwater BGA content. This information is essential for improving our currently limited understanding of the potentially wide ranging atmospheric impacts of LSA, particularly in regions with large freshwater surface area, high wind speeds, and increasing HAB severity, such as the Great Lakes.[43,62,63] The identification of biological material associated with individual LSA particles and its relation to BGA concentration in this study demonstrates that freshwater wave breaking should be further studied as a vector for the introduction of aquatic toxins into the atmosphere. The LSA-Bio ATOFMS spectra characterized in this study could thus be used in future field measurements to identify the presence in the ambient atmosphere of potentially toxic bioaerosols produced by wave breaking induced bubble bursting from freshwater containing HABs. However, as the species present in freshwater algal blooms can range in toxicity,[64] LSA produced by wave breaking induced bubble bursting from freshwater containing HABs also needs to be studied with techniques that can assess the molecular composition and toxicity of HAB products present to fully assess the public health impacts of freshwater wave breaking.[65,66]

The identification of biological material associated with individual LSA particles demonstrates freshwater wave breaking as a potentially important process for the introduction of freshwater biological INP into the atmosphere.[37,38,67] The relative enrichment of organic compounds in smaller diameter LSA, similar to SSA, is also important to consider in predicting cloud droplet formation. Previous SSA studies have concluded that particles composed mostly of hygroscopic salts will activate into cloud drops at relatively smaller sizes, with the addition of less soluble organic species decreasing the overall hygroscopicity and increasing the size at which the particles can activate.[9] However, studies on the effect of the distribution of inorganic and organic material on the hygroscopic properties of SSA may not be able to fully predict LSA climate impacts because of the differences in inorganic and organic species and associated concentrations present between freshwater and seawater.[27] Laboratory measurements of the relationship between freshwater biological activity and LSA INP and CCN activity are needed to improve prediction of LSA climate impacts in models. In addition, field measurements of the size-dependent fluxes of LSA, including those particles containing biological material, from the freshwater to the atmosphere need to be conducted across various stages of freshwater algal bloom development to improve understanding of LSA production and air quality model simulations.

■ ASSOCIATED CONTENT

Supporting Information

The Supporting Information is available free of charge on the ACS Publications website at DOI: 10.1021/acs.est.7b03609.

Additional results and discussion of the prefreeze and freeze−thaw comparison experiment using the 2017 Lake Erie − Maumee freshwater sample. Additional sampling region satellite imagery, measured aerosol size distributions, optical, and fluorescence imaging, mass spectral subtraction plots, and particle circularity distributions (PDF)

■ AUTHOR INFORMATION

Corresponding Authors

*(K.A.P.) E-mail: prattka@umich.edu.
*(A.P.A.) E-mail: aulta@umich.edu.

ORCID

Swarup China: 0000-0001-7670-335X
Alexander Laskin: 0000-0002-7836-8417
Andrew P. Ault: 0000-0002-7313-8559
Kerri A. Pratt: 0000-0003-4707-2290

Present Address

⊥(A.L.) Department of Chemistry, Purdue University, West Lafayette, Indiana 47907−2084, United States

Notes

The authors declare no competing financial interest.

■ ACKNOWLEDGMENTS

The University of Michigan Water Center provided funding for freshwater collection. SEM-EDX analyses were performed at the Environmental Molecular Sciences Laboratory (EMSL), a national scientific user facility located at the Pacific Northwest National Laboratory (PNNL) and sponsored by the Office of Biological and Environmental Research of the U.S Department of Energy (DOE). PNNL is operated for DOE by Battelle Memorial Institute under Contract No. DE-AC06-76RL0 1830. N.E. O.'s travel to PNNL was partially supported by a University of Michigan Rackham Graduate School Research Grant. J.L. A. was partially supported through the University of Michigan Dow Sustainability Postdoctoral Fellows Program. M.P. was supported by the University of Michigan, Department of Chemistry National Science Foundation Research Experience for Undergraduates program (CHE-1460990). K. Prather and J. Mayer (Univ. of California, San Diego) are thanked for the designs and assistance in building the ATOFMS.

■ REFERENCES

(1) Smith, V. H. Eutrophication of freshwater and coastal marine ecosystems a global problem. *Environ. Sci. Pollut. Res.* **2003**, *10* (2), 126−139.

(2) Carmichael, W. W.; Boyer, G. L. Health impacts from cyanobacteria harmful algae blooms: Implications for the North American Great Lakes. *Harmful Algae* **2016**, *54*, 194−212.

(3) Kirkpatrick, B.; Fleming, L. E.; Bean, J. A.; Nierenberg, K.; Backer, L. C.; Cheng, Y. S.; Pierce, R.; Reich, A.; Naar, J.; Wanner, A.; Abraham, W. M.; Zhou, Y.; Hollenbeck, J.; Baden, D. G. Aerosolized Red Tide Toxins (Brevetoxins) and Asthma: Continued health effects after 1 h beach exposure. *Harmful Algae* **2011**, *10* (2), 138−143.

(4) Cheng, Y. S.; Villareal, T. A.; Zhou, Y.; Gao, J.; Pierce, R.; Naar, J.; Baden, D. G. Characterization of Red Tide Aerosol on the Texas Coast. *Harmful Algae* **2005**, *4* (1), 87−94.

DOI: 10.1021/acs.est.7b03609
Environ. Sci. Technol. 2018, 52, 397−405

(5) Backer, L. C.; McNeel, S. V.; Barber, T.; Kirkpatrick, B.; Williams, C.; Irvin, M.; Zhou, Y.; Johnson, T. B.; Nierenberg, K.; Aubel, M.; LePrell, R.; Chapman, A.; Foss, A.; Corum, S.; Hill, V. R.; Kieszak, S. M.; Cheng, Y. S. Recreational exposure to microcystins during algal blooms in two California lakes. *Toxicon* **2010**, *55* (5), 909−21.
(6) Backer, L. C.; Carmichael, W.; Kirkpatrick, B.; Williams, C.; Irvin, M.; Zhou, Y.; Johnson, T. B.; Nierenberg, K.; Hill, V. R.; Kieszak, S. M.; Cheng, Y. S. Recreational exposure to low concentrations of microcystins during an algal bloom in a small lake. *Mar. Drugs* **2008**, *6* (2), 389−406.
(7) Axson, J. L.; May, N. W.; Colon-Bernal, I. D.; Pratt, K. A.; Ault, A. P. Lake Spray Aerosol: A Chemical Signature from Individual Ambient Particles. *Environ. Sci. Technol.* **2016**, *50* (18), 9835−45.
(8) Quinn, P. K.; Collins, D. B.; Grassian, V. H.; Prather, K. A.; Bates, T. S. Chemisstry and related properties of freshly emitted sea spray aerosol. *Chem. Rev.* **2015**, *115* (10), 4383−99.
(9) Prather, K. A.; Bertram, T. H.; Grassian, V. H.; Deane, G. B.; Stokes, M. D.; Demott, P. J.; Aluwihare, L. I.; Palenik, B. P.; Azam, F.; Seinfeld, J. H.; Moffet, R. C.; Molina, M. J.; Cappa, C. D.; Geiger, F. M.; Roberts, G. C.; Russell, L. M.; Ault, A. P.; Baltrusaitis, J.; Collins, D. B.; Corrigan, C. E.; Cuadra-Rodriguez, L. A.; Ebben, C. J.; Forestieri, S. D.; Guasco, T. L.; Hersey, S. P.; Kim, M. J.; Lambert, W. F.; Modini, R. L.; Mui, W.; Pedler, B. E.; Ruppel, M. J.; Ryder, O. S.; Schoepp, N. G.; Sullivan, R. C.; Zhao, D. Bringing the ocean into the laboratory to probe the chemical complexity of sea spray aerosol. *Proc. Natl. Acad. Sci. U. S. A.* **2013**, *110* (19), 7550−5.
(10) Facchini, M. C.; Rinaldi, M.; Decesari, S.; Carbone, C.; Finessi, E.; Mircea, M.; Fuzzi, S.; Ceburnis, D.; Flanagan, R.; Nilsson, E. D.; de Leeuw, G.; Martino, M.; Woeltjen, J.; O'Dowd, C. D. Primary submicron marine aerosol dominated by insoluble organic colloids and aggregates, *Geophys. Res. Lett.*, **2008**, *35*, (17);10.1029/2008GL034210.
(11) O'Dowd, C. D.; Facchini, M. C.; Cavalli, F.; Ceburnis, D.; Mircea, M.; Decesari, S.; Fuzzi, S.; Yoon, Y. J.; Putaud, J. P. Biogenically driven organic contribution to marine aerosol. *Nature* **2004**, *431* (7009), 676−80.
(12) Keene, W. C.; Maring, H.; Maben, J. R.; Kieber, D. J.; Pszenny, A. A. P.; Dahl, E. E.; Izaguirre, M. A.; Davis, A. J.; Long, M. S.; Zhou, X. L.; Smoydzin, L.; Sander, R. Chemical and physical characteristics of nascent aerosols produced by bursting bubbles at a model air-sea interface, *J. Geophys. Res.*, **2007**, *112*, (D21);10.1029/2007JD008464.
(13) Bigg, E. K.; Leck, C. The composition of fragments of bubbles bursting at the ocean surface, *J. Geophys. Res.*, **2008**, *113*, (D11); 10.1029/2007JD009078.
(14) Zhang, Z. Direct determination of thickness of sea surface microlayer using a pH microelectrode at original location. *Sci. China, Ser. B: Chem.* **2003**, *46* (4), 339.
(15) Hawkins, L. N.; Russell, L. M. Polysaccharides, Proteins, and Phytoplankton Fragments: Four Chemically Distinct Types of Marine Primary Organic Aerosol Classified by Single Particle Spectromicroscopy. *Adv. Meteorol.* **2010**, *2010*, 1−14.
(16) Blanchard, D. C.; Syzdek, L. D. Electrostatic collection of jet and film drops. *Limnol. Oceanogr.* **1975**, *20* (5), 762−774.
(17) Meyers, P. A.; Kawka, O. E. Fractionation of Hydrophobic Organic Materials in Surface Microlayers. *J. Great Lakes Res.* **1982**, *8* (2), 288−298.
(18) Fuhs, G. W. Microbiota in Surface Films: an Historical Perspective. *J. Great Lakes Res.* **1982**, *8* (2), 312−315.
(19) Andren, A. W.; Elzerman, A. W.; Armstrong, D. E. Chemical and Physical Aspects of Surface Organic Microlayers in Freshwater Lakes. *J. Great Lakes Res.* **1976**, *2*, 101−110.
(20) Shuchman, R. A.; Leshkevich, G.; Sayers, M. J.; Johengen, T. H.; Brooks, C. N.; Pozdnyakov, D. An algorithm to retrieve chlorophyll, dissolved organic carbon, and suspended minerals from Great Lakes satellite data. *J. Great Lakes Res.* **2013**, *39*, 14−33.
(21) Biddanda, B. A.; Cotner, J. B. Love Handles in Aquatic Ecosystems: The Role of Dissolved Organic Carbon Drawdown, Resuspended Sediments, and Terrigenous Inputs in the Carbon Balance of Lake Michigan. *Ecosystems* **2002**, *5* (5), 431−445.
(22) Repeta, D. J.; Quan, T. M.; Aluwihare, L. I.; Accardi, A. Chemical characterization of high molecular weight dissolved organic matter in fresh and marine waters. *Geochim. Cosmochim. Acta* **2002**, *66* (6), 955−962.
(23) Cory, R. M.; Davis, T. W.; Dick, G. J.; Johengen, T.; Denef, V. J.; Berry, M. A.; Page, S. E.; Watson, S. B.; Yuhas, K.; Kling, G. W. Seasonal Dynamics in Dissolved Organic Matter, Hydrogen Peroxide, and Cyanobacterial Blooms in Lake Erie, *Front. Mar. Sci.*, **2016**, *3*, 10.3389/fmars.2016.00054.
(24) Ittekkot, V. Variations of dissolved organic matter during a plankton bloom: qualitative aspects, based on sugar and amino acid analyses. *Mar. Chem.* **1982**, *11* (2), 143−158.
(25) Pilson, M. E. Q. *An Introduction to the Chemistry of the Sea*, 2 ed.; Cambridge University Press: Cambridge, 2013.
(26) Chapra, S. C.; Dove, A.; Warren, G. J. Long-term trends of Great Lakes major ion chemistry. *J. Great Lakes Res.* **2012**, *38* (3), 550−560.
(27) May, N. W.; Axson, J. L.; Watson, A.; Pratt, K. A.; Ault, A. P. Lake spray aerosol generation: a method for producing representative particles from freshwater wave breaking. *Atmos. Meas. Tech.* **2016**, *9* (9), 4311−4325.
(28) Forestieri, S. D.; Cornwell, G. C.; Helgestad, T. M.; Moore, K. A.; Lee, C.; Novak, G. A.; Sultana, C. M.; Wang, X.; Bertram, T. H.; Prather, K. A.; Cappa, C. D. Linking variations in sea spray aerosol particle hygroscopicity to composition during two microcosm experiments. *Atmos. Chem. Phys.* **2016**, *16* (14), 9003−9018.
(29) Andreae, M. O.; Rosenfeld, D. Aerosol−cloud−precipitation interactions. Part 1. The nature and sources of cloud-active aerosols. *Earth-Sci. Rev.* **2008**, *89* (1−2), 13−41.
(30) Matthias-Maser, S.; Brinkmann, J.; Schneider, W. The size distribution of marine atmospheric aerosol with regard to primary biological aerosol particles over the South Atlantic Ocean. *Atmos. Environ.* **1999**, *33* (21), 3569−3575.
(31) Aller, J. Y.; Kuznetsova, M. R.; Jahns, C. J.; Kemp, P. F. The sea surface microlayer as a source of viral and bacterial enrichment in marine aerosols. *J. Aerosol Sci.* **2005**, *36* (5−6), 801−812.
(32) McCluskey, C. S.; Hill, T. C. J.; Malfatti, F.; Sultana, C. M.; Lee, C.; Santander, M. V.; Beall, C. M.; Moore, K. A.; Cornwell, G. C.; Collins, D. B.; Prather, K. A.; Jayarathne, T.; Stone, E. A.; Azam, F.; Kreidenweis, S. M.; DeMott, P. J. A Dynamic Link between Ice Nucleating Particles Released in Nascent Sea Spray Aerosol and Oceanic Biological Activity during Two Mesocosm Experiments. *J. Atmos. Sci.* **2017**, *74* (1), 151−166.
(33) Vergara-Temprado, J.; Murray, B. J.; Wilson, T. W.; amp; apos; Sullivan, D.; Browse, J.; Pringle, K. J.; Ardon-Dryer, K.; Bertram, A. K.; Burrows, S. M.; Ceburnis, D.; DeMott, P. J.; Mason, R. H.; amp; apos; Dowd, C. D.; Rinaldi, M.; Carslaw, K. S. Contribution of feldspar and marine organic aerosols to global ice nucleating particle concentrations. *Atmos. Chem. Phys.* **2017**, *17* (5), 3637−3658.
(34) DeMott, P. J.; Hill, T. C.; McCluskey, C. S.; Prather, K. A.; Collins, D. B.; Sullivan, R. C.; Ruppel, M. J.; Mason, R. H.; Irish, V. E.; Lee, T.; Hwang, C. Y.; Rhee, T. S.; Snider, J. R.; McMeeking, G. R.; Dhaniyala, S.; Lewis, E. R.; Wentzell, J. J.; Abbatt, J.; Lee, C.; Sultana, C. M.; Ault, A. P.; Axson, J. L.; Diaz Martinez, M.; Venero, I.; Santos-Figueroa, G.; Stokes, M. D.; Deane, G. B.; Mayol-Bracero, O. L.; Grassian, V. H.; Bertram, T. H.; Bertram, A. K.; Moffett, B. F.; Franc, G. D. Sea spray aerosol as a unique source of ice nucleating particles. *Proc. Natl. Acad. Sci. U. S. A.* **2016**, *113* (21), 5797−803.
(35) Wilson, T. W.; Ladino, L. A.; Alpert, P. A.; Breckels, M. N.; Brooks, I. M.; Browse, J.; Burrows, S. M.; Carslaw, K. S.; Huffman, J. A.; Judd, C.; Kilthau, W. P.; Mason, R. H.; McFiggans, G.; Miller, L. A.; Najera, J. J.; Polishchuk, E.; Rae, S.; Schiller, C. L.; Si, M.; Temprado, J. V.; Whale, T. F.; Wong, J. P.; Wurl, O.; Yakobi-Hancock, J. D.; Abbatt, J. P.; Aller, J. Y.; Bertram, A. K.; Knopf, D. A.; Murray, B. J. A marine biogenic source of atmospheric ice-nucleating particles. *Nature* **2015**, *525* (7568), 234−8.
(36) Ladino, L. A.; Yakobi-Hancock, J. D.; Kilthau, W. P.; Mason, R. H.; Si, M.; Li, J.; Miller, L. A.; Schiller, C. L.; Huffman, J. A.; Aller, J. Y.; Knopf, D. A.; Bertram, A. K.; Abbatt, J. P. D. Addressing the ice

DOI: 10.1021/acs.est.7b03609
Environ. Sci. Technol. 2018, 52, 397−405

nucleating abilities of marine aerosol: A combination of deposition mode laboratory and field measurements. *Atmos. Environ.* **2016**, *132*, 1−10.
(37) D'Souza N, A.; Kawarasaki, Y.; Gantz, J. D.; Lee, R. E., Jr.; Beall, B. F.; Shtarkman, Y. M.; Kocer, Z. A.; Rogers, S. O.; Wildschutte, H.; Bullerjahn, G. S.; McKay, R. M. Diatom assemblages promote ice formation in large lakes. *ISME J.* **2013**, *7* (8), 1632−40.
(38) Moffett, B. F. Fresh water ice nuclei. *Fundam. Appl. Limnol.* **2016**, *188* (1), 19−23.
(39) Collins, D. B.; Zhao, D. F.; Ruppel, M. J.; Laskina, O.; Grandquist, J. R.; Modini, R. L.; Stokes, M. D.; Russell, L. M.; Bertram, T. H.; Grassian, V. H.; Deane, G. B.; Prather, K. A. Direct aerosol chemical composition measurements to evaluate the physicochemical differences between controlled sea spray aerosol generation schemes. *Atmos. Meas. Tech.* **2014**, *7* (11), 3667−3683.
(40) Guasco, T. L.; Cuadra-Rodriguez, L. A.; Pedler, B. E.; Ault, A. P.; Collins, D. B.; Zhao, D.; Kim, M. J.; Ruppel, M. J.; Wilson, S. C.; Pomeroy, R. S.; Grassian, V. H.; Azam, F.; Bertram, T. H.; Prather, K. A. Transition metal associations with primary biological particles in sea spray aerosol generated in a wave channel. *Environ. Sci. Technol.* **2014**, *48* (2), 1324−33.
(41) Collins, D. B.; Ault, A. P.; Moffet, R. C.; Ruppel, M. J.; Cuadra-Rodriguez, L. A.; Guasco, T. L.; Corrigan, C. E.; Pedler, B. E.; Azam, F.; Aluwihare, L. I.; Bertram, T. H.; Roberts, G. C.; Grassian, V. H.; Prather, K. A. Impact of marine biogeochemistry on the chemical mixing state and cloud forming ability of nascent sea spray aerosol. *J. Geophys. Res. Atmos.* **2013**, *118* (15), 8553−8565.
(42) Steffen, M. M.; Belisle, B. S.; Watson, S. B.; Boyer, G. L.; Wilhelm, S. W. Status, causes and controls of cyanobacterial blooms in Lake Erie. *J. Great Lakes Res.* **2014**, *40* (2), 215−225.
(43) Doubrawa, P.; Barthelmie, R. J.; Pryor, S. C.; Hasager, C. B.; Badger, M.; Karagali, I. Satellite winds as a tool for offshore wind resource assessment: The Great Lakes Wind Atlas. *Remote Sens. Environ.* **2015**, *168*, 349−359.
(44) Marion, J. W.; Lee, J.; Wilkins, J. R., 3rd; Lemeshow, S.; Lee, C.; Waletzko, E. J.; Buckley, T. J. In vivo phycocyanin flourometry as a potential rapid screening tool for predicting elevated microcystin concentrations at eutrophic lakes. *Environ. Sci. Technol.* **2012**, *46* (8), 4523−31.
(45) Fuentes, E.; Coe, H.; Green, D.; de Leeuw, G.; McFiggans, G. Laboratory-generated primary marine aerosol via bubble-bursting and atomization. *Atmos. Meas. Tech.* **2010**, *3* (1), 141−162.
(46) Neubauer, K. R.; Johnston, M. V.; Wexler, A. S. On-line analysis of aqueous aerosols by laser desorption ionization. *Int. J. Mass Spectrom. Ion Processes* **1997**, *163* (1−2), 29−37.
(47) Pratt, K. A.; Mayer, J. E.; Holecek, J. C.; Moffet, R. C.; Sanchez, R. O.; Rebotier, T. P.; Furutani, H.; Gonin, M.; Fuhrer, K.; Su, Y.; Guazzotti, S.; Prather, K. A. Development and characterization of an aircraft aerosol time-of-flight mass spectrometer. *Anal. Chem.* **2009**, *81* (5), 1792−800.
(48) Cahill, J. F.; Darlington, T. K.; Fitzgerald, C.; Schoepp, N. G.; Beld, J.; Burkart, M. D.; Prather, K. A. Online analysis of single cyanobacteria and algae cells under nitrogen-limited conditions using aerosol time-of-flight mass spectrometry. *Anal. Chem.* **2015**, *87* (16), 8039−46.
(49) Sultana, C. M.; Cornwell, G. C.; Rodriguez, P.; Prather, K. A. FATES: a flexible analysis toolkit for the exploration of single-particle mass spectrometer data. *Atmos. Meas. Tech.* **2017**, *10* (4), 1323−1334.
(50) Lee, C.; Sultana, C. M.; Collins, D. B.; Santander, M. V.; Axson, J. L.; Malfatti, F.; Cornwell, G. C.; Grandquist, J. R.; Deane, G. B.; Stokes, M. D.; Azam, F.; Grassian, V. H.; Prather, K. A. Advancing Model Systems for Fundamental Laboratory Studies of Sea Spray Aerosol Using the Microbial Loop. *J. Phys. Chem. A* **2015**, *119* (33), 8860−70.
(51) Russell, S. C.; Czerwieniec, G.; Lebrilla, C.; Tobias, H.; Fergenson, D. P.; Steele, P.; Pitesky, M.; Horn, J.; Srivastava, A.; Frank, M.; Gard, E. E. Toward understanding the ionization of biomarkers from micrometer particles by bio-aerosol mass spectrometry. *J. Am. Soc. Mass Spectrom.* **2004**, *15* (6), 900−9.
(52) Pratt, K. A.; DeMott, P. J.; French, J. R.; Wang, Z.; Westphal, D. L.; Heymsfield, A. J.; Twohy, C. H.; Prenni, A. J.; Prather, K. A. In situ detection of biological particles in cloud ice-crystals. *Nat. Geosci.* **2009**, *2* (6), 398−401.
(53) Sultana, C. M.; Al-Mashat, H.; Prather, K. A. Expanding Single Particle Mass Spectrometer Analyses for the Identification of Microbe Signatures in Sea Spray Aerosol. *Anal. Chem.* **2017**, *89* (19), 10162−10170.
(54) Yan, Y.-d.; Jameson, G. J. Application of the Jameson Cell technology for algae and phosphorus removal from maturation ponds. *Int. J. Miner. Process.* **2004**, *73* (1), 23−28.
(55) Mensah-Attipoe, J.; Saari, S.; Veijalainen, A. M.; Pasanen, P.; Keskinen, J.; Leskinen, J. T.; Reponen, T. Release and characteristics of fungal fragments in various conditions. *Sci. Total Environ.* **2016**, *547*, 234−43.
(56) Ault, A. P.; Moffet, R. C.; Baltrusaitis, J.; Collins, D. B.; Ruppel, M. J.; Cuadra-Rodriguez, L. A.; Zhao, D.; Guasco, T. L.; Ebben, C. J.; Geiger, F. M.; Bertram, T. H.; Prather, K. A.; Grassian, V. H. Size-dependent changes in sea spray aerosol composition and properties with different seawater conditions. *Environ. Sci. Technol.* **2013**, *47* (11), 5603−12.
(57) Patterson, J. P.; Collins, D. B.; Michaud, J. M.; Axson, J. L.; Sultana, C. M.; Moser, T.; Dommer, A. C.; Conner, J.; Grassian, V. H.; Stokes, M. D.; Deane, G. B.; Evans, J. E.; Burkart, M. D.; Prather, K. A.; Gianneschi, N. C. Sea Spray Aerosol Structure and Composition Using Cryogenic Transmission Electron Microscopy. *ACS Cent. Sci.* **2016**, *2* (1), 40−47.
(58) Blanchard, D. C.; Syzdek, L. D. Concentration of bacteria in jet drops from bursting bubbles. *J. Geophys. Res.* **1972**, *77* (27), 5087−5099.
(59) Kientzler, C. F.; Arons, A. B.; Blanchard, D. C.; Woodcock, A. H. Photographic Investigation of the Projection of Droplets by Bubbles Bursting at a Water Surface. *Tellus* **1954**, *6* (1), 1−7.
(60) Lewis, E. R.; Schwartz, S. E. *Sea Salt Aerosol Production: Mechanisms, Methods, Measurements, and Models - A Critical Review*; American Geophysical Union: Washington D.C., 2004; Vol. *152*.
(61) Pöhlker, C.; Huffman, J. A.; Pöschl, U. Autofluorescence of atmospheric bioaerosols − fluorescent biomolecules and potential interferences. *Atmos. Meas. Tech.* **2012**, *5* (1), 37−71.
(62) Chung, S. H.; Basarab, B. M.; VanReken, T. M. Regional impacts of ultrafine particle emissions from the surface of the Great Lakes. *Atmos. Chem. Phys.* **2011**, *11* (24), 12601−12615.
(63) Michalak, A. M.; Anderson, E. J.; Beletsky, D.; Boland, S.; Bosch, N. S.; Bridgeman, T. B.; Chaffin, J. D.; Cho, K.; Confesor, R.; Daloglu, I.; Depinto, J. V.; Evans, M. A.; Fahnenstiel, G. L.; He, L.; Ho, J. C.; Jenkins, L.; Johengen, T. H.; Kuo, K. C.; Laporte, E.; Liu, X.; McWilliams, M. R.; Moore, M. R.; Posselt, D. J.; Richards, R. P.; Scavia, D.; Steiner, A. L.; Verhamme, E.; Wright, D. M.; Zagorski, M. A. Record-setting algal bloom in Lake Erie caused by agricultural and meteorological trends consistent with expected future conditions. *Proc. Natl. Acad. Sci. U. S. A.* **2013**, *110* (16), 6448−52.
(64) Gobler, C. J.; Burkholder, J. M.; Davis, T. W.; Harke, M. J.; Johengen, T.; Stow, C. A.; Van de Waal, D. B. The dual role of nitrogen supply in controlling the growth and toxicity of cyanobacterial blooms. *Harmful Algae* **2016**, *54*, 87−97.
(65) Gambaro, A.; Barbaro, E.; Zangrando, R.; Barbante, C. Simultaneous quantification of microcystins and nodularin in aerosol samples using high-performance liquid chromatography/negative electrospray ionization tandem mass spectrometry. *Rapid Commun. Mass Spectrom.* **2012**, *26* (12), 1497−506.
(66) Msagati, T. A.; Siame, B. A.; Shushu, D. D. Evaluation of methods for the isolation, detection and quantification of cyanobacterial hepatotoxins. *Aquat. Toxicol.* **2006**, *78* (4), 382−97.
(67) Pietsch, R. B.; David, R. F.; Marr, L. C.; Vinatzer, B.; Schmale, D. G. Aerosolization of Two Strains (Ice+ and Ice−) ofPseudomonas syringaein a Collison Nebulizer at Different Temperatures. *Aerosol Sci. Technol.* **2015**, *49* (3), 159−166.

DOI: 10.1021/acs.est.7b03609
Environ. Sci. Technol. 2018, 52, 397−405